

University of Mississippi

eGrove

Honors Theses

Honors College (Sally McDonnell Barksdale
Honors College)

2007

Cruciform Extrusion in Methylation-State Variants of pBR322 Plasmid

Lucas Morgan McElwain

Follow this and additional works at: https://egrove.olemiss.edu/hon_thesis

Recommended Citation

McElwain, Lucas Morgan, "Cruciform Extrusion in Methylation-State Variants of pBR322 Plasmid" (2007). *Honors Theses*. 2236.

https://egrove.olemiss.edu/hon_thesis/2236

This Undergraduate Thesis is brought to you for free and open access by the Honors College (Sally McDonnell Barksdale Honors College) at eGrove. It has been accepted for inclusion in Honors Theses by an authorized administrator of eGrove. For more information, please contact egrove@olemiss.edu.

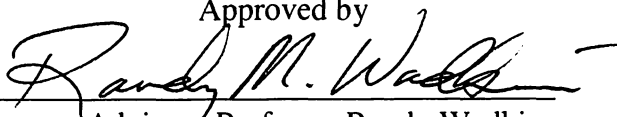
CRUCIFORM EXTRUSION IN METHYLATION-STATE VARIANTS OF pBR322
PLASMID

by
Lucas Morgan McElwain

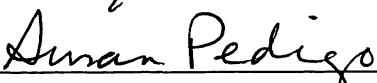
A thesis submitted to the faculty of the University of Mississippi in partial fulfillment of
the requirements of the Sally McDonnell Barksdale Honors College

Oxford
May 2007

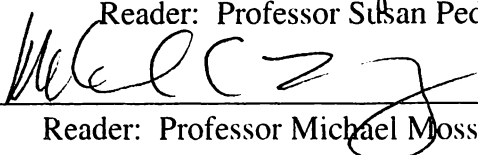
Approved by



Advisor: Professor Randy Wadkins



Reader: Professor Susan Pedigo



Reader: Professor Michael Mossing

ACKNOWLEDGEMENT

I recognize Dr. Wadkins for his patient instruction and guidance over the duration of this project. I also appreciate the friendship of other researchers under Dr. Wadkins—Yi “Ally” Chen, Xu Zhang, and Xiaozhen “Shawn” Yu. Thanks to W.H. Freeman and Co. for use of figures from the *Leninger* text.

ABSTRACT

LUCAS MORGAN MCELWAIN: Cruciform Extrusion in Methylation-State Variants of pBR322 Plasmid

(Under the direction of Assistant Professor Randy M. Wadkins)

The presence of DNA secondary structures in genomic DNA has been observed in both prokaryotes and eukaryotes. Specifically, sections of ssDNA may melt out and form cruciform/hairpin structures within palindromic sequences or areas of high purine content. Negative supercoiling of the DNA is necessary for energetic favorability of such an event. These noncanonical structures may serve as molecular switches, providing additional regulation of DNA transactions such as transcription and perhaps replication and recombination. Secondary structures associated with regulatory regions are of particular interest as potential sites for the binding of small molecules, which could alter the expression of genes. The effect of system-wide DNA base methylation on extrusion of secondary structures is one aspect of primary-secondary-tertiary structure interplay that has not been examined. Our study first characterized the gross qualitative effect of methylation of plasmid DNA on the formation of cruciform structures. The plasmid pBR322 was transformed into three different strains of *E. coli*: K12 with functional deoxycytosine and deoxyadenine methyltransferases, BL21 strain (*dcm*⁻), and K12 ER2925 with no methyltransferase activity (*dam*⁻/*dcm*⁻). The resulting purified plasmids were then digested with mung bean nuclease (MBN); a ssDNA-specific nuclease; and then by a site-specific nuclease. The digest reaction mixtures were

analyzed by gel electrophoresis for fragments characteristic of cleavage by MBN. The three strains seemed to show no difference in the presence of at least one prominent ssDNA site. Topoisomers of each plasmid were then created by the relaxation of negative supercoils in the presence of DNA intercalator and separated through gel electrophoresis. The three methylation-state variants seemed to exhibit similar structural responses. These data indicate that methylation of respective nucleotide bases does not seem to influence cruciform extrusion, through either changes in local or global conformations.

TABLE OF CONTENTS

LIST OF FIGURES	vi
LIST OF ABBREVIATIONS	vii
INTRODUCTION	
1.1 Occurrence and Relevance of ssDNA.....	1
1.2 Systemic Considerations.....	6
1.3 Base Methylation	7
1.4 Aims and Approach	10
1.4.1 Topology Review.....	11
1.4.2 Experimental System	14
MATERIALS AND METHODS	
2.1 Plasmids	15
2.2 Endonuclease Restriction.....	17
2.3 Topoisomer Production.....	19
2.4 Buffers and Media.....	20
RESULTS	
3.1 Mung Bean Nuclease Cleavage Patterns Among pBR322 Variant Plasmids.....	23
3.2 Topoisomers and Relative Superhelical Conformation	27
DISCUSSION	36
LIST OF REFERENCES	39

LIST OF FIGURES

Figure 1	Towards Extrusion of Cruciform Secondary Structure in DNA.....	2
Figure 2	Palindromic Sequences Allow Shift in Structure of DNA.....	2
Figure 3	Methylated Nucleotides	9
Figure 4	Accommodation of Decreased <i>Lk</i> by Supercoiling	12
Figure 5	Illustration of Topological Concepts and Terms	13
Figure 6	Area of Interest in Terminator Region of Amp-R Gene.....	23
Figure 7	Basic Map of pBR322 Plasmid and Restriction Products	24
Figure 8	Gel Electrophoresis Image of MBN Digestion Results	26
Figure 9	Effect of Intercalator Addition upon ccDNA Topology and Gel Electrophoresis Mobility.....	29
Figure 10	Gel Image of Topoisomer Production in K12 pBR322	31
Figure 11	Gel Image of Topoisomer Production in K12 pBR322 + EtBr	32
Figure 12	Relative Intensity/Mobility Tracings of Topoisomers from K12 pBR322	33
Figure 13	Gel Images of Topoisomer Production in <i>dcm</i> ⁻ and <i>dam</i> ⁻ / <i>dcm</i> ⁻ pBR322.....	34
Figure 14	Comparison of Changes in Supercoiling by Intercalator Concentration	35

LIST OF ABBREVIATIONS

AGE	agarose gel electrophoresis
Amp-R	ampicillin resistance
BL21	<i>E. coli</i> strain with defective cytosine methylase (hemimethylated; <i>dcm</i> ⁻)
ccDNA	closed circular DNA
<i>dam</i> ⁻	DNA adenine methylase (defective gene)
<i>dcm</i> ⁻	DNA cytosine methylase (defective gene)
dsDNA	double stranded DNA
ER2925	<i>E. coli</i> K12 strain with defective adenine and cytosine methylases (<i>dam</i> ⁻ / <i>dcm</i> ⁻)
EtBr	ethidium bromide
K12	<i>E. coli</i> strain with functional methylases
kb	kilobases
<i>Lk</i>	linking number
MBN	mung bean nuclease
σ	superhelical density
ssDNA	single stranded DNA
Topo 1	human Topoisomerase I
VPD	venom phosphodiesterase

INTRODUCTION

The function of DNA as a coding template for all life processes requires that it be accessible for transcription of its information and replication of itself. At the same time, this linear molecule of thousands to billions of base pairs must be packaged compactly within a nucleus that is usually microscopic. By manipulating local and global organization of DNA structure, cells address both its spatial processing and its accessibility.

1. 1 Occurrence and Relevance of ssDNA

Structural strain induced by endogenous underwinding of DNA may affect changes in local secondary structure. Not long after the discovery of the double helix, researchers visualized the possibility of the extrusion of single-stranded DNA (ssDNA) [Platt 1955]. Such melting out of the DNA should occur especially in torsionally stressed regions having two-fold symmetry of base sequence to form cruciform structures (Figure 1). Such inverted repeats, or palindromes, are self-complementary (Figure 2), and their extrusion and subsequent intrastrand pairing may be energetically favorable in highly supercoiled DNA.

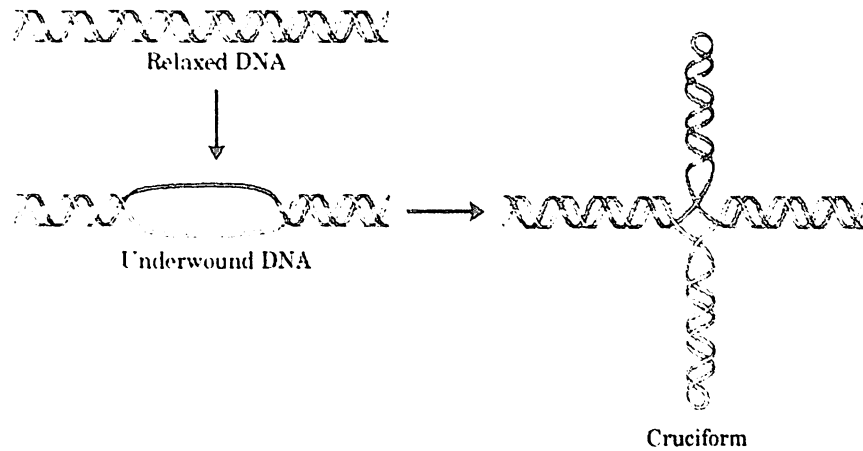


Figure 1: Towards Extrusion of Cruciform Secondary Structure in DNA. Source: Nelson, D. L.; Cox, M. M. Leninger Principles of Biochemistry, 3rd ed. New York: W. H. Freeman and Co., 2000. Fig 24-18. Relaxed DNA (top left) may be underwound *in vivo* (bottom left). The stressed molecule may then reanneal to form the more stable noncanonical secondary structures such as the cruciform.

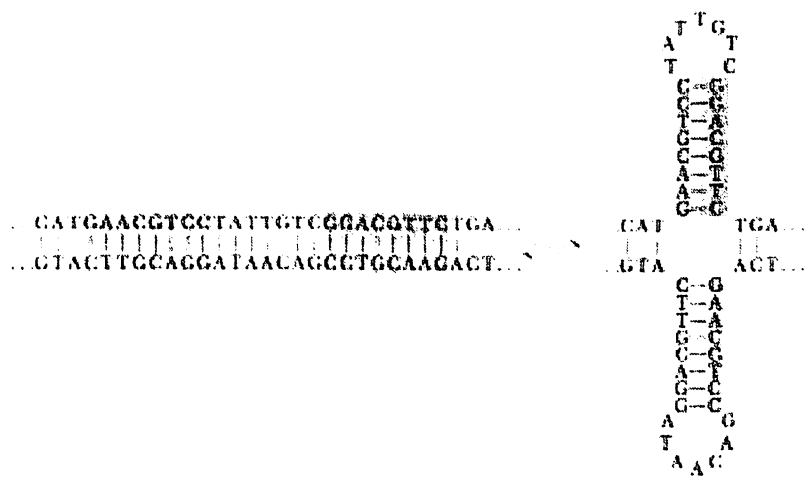


Figure 2: Palindromic Sequences Allow Shift in Structure of DNA. Source: <http://www.web.virginia.edu/Heidi/Chapter12/Images/>. Base pairing is retained in the majority of this cruciform (stem region), but regions of ssDNA remain due to sterical hindrance and noncomplementary bases (loop region).

A free energy increase in supercoiled DNA relative to relaxed DNA results from the action of gyrase in prokaryotes or transcription machinery such as polymerases and is given by the equation:

$$\Delta G_S = (KRT/N)\Delta Lk^2$$

where K is a proportionality constant equal to 1100 for molecules over 2Kb, R is the gas constant, T the absolute temperature, and ΔLk the number of superhelical turns [Lilley 1985; Palecek 1991]. The free energy in supercoiled DNA is relieved by the favorable decrease in Lk when a cruciform is extruded. Additionally, the unpaired bases at the loops of cruciforms means a loss of base pairing, which further relieves the negative supercoiling energy [reviewed in Wadkins 2000].

Lilley produced some of the first experimental evidence showing that cruciform structures form in supercoiled plasmid DNA (1980). Subsequently, evidence has been produced to support the occurrence of such secondary structures also occur *in vivo* [Pearson 1996; Leach 1994]. Single-strand specific nucleases such as S1 and mung bean nuclease selectively act in polypurine-polypyrimidine tracts such as are found in gene borders in the genomic dsDNA of various eukaryotes. Additionally, heteropolypurine regions form stable hairpins maintained by non-Watson-Crick base pairing between adenine and guanine. Further experiments indicated that these structures form preferentially on gene borders in both prokaryotes and eukaryotes. Mung bean nuclease excises entire genes in the genomic DNA of *P. falciparum*, with cleavage sites outside of the actual coding region. Transposed *Drosophila* heat shock genes are cleaved by single-strand specific nuclease upstream of the genes in purine populated sequences (reviewed in Wadkins 2000).

Though Nelson purports that these secondary structures are “of less physiological importance than ” the induction of strand separation by supercoiling [Nelson 2005], such conservation of these regions containing ssDNA hints at a role for noncanonical structures in gene regulation, namely during transcription. Cleavage sites for single-strand specific DNA nucleases occur within promoters of the RNA primer for DNA replication, in promoters for ampicillin- and tetracycline-resistance cassettes, and in the terminator of the ampicillin-resistance gene in otherwise double-stranded *E. coli* plasmid pBR322 [Sheflin 1985]. Similarly, mung bean nuclease acts on supercoiled, but not relaxed, SV40 DNA. Cleavage occurs at transcriptional enhancers and upstream of transcriptional start sites corresponding to regions of short inverted repeats, and varies with divalent salt concentration [Iacono-Connors 1986]. These data suggest a regulatory role of ssDNA-containing secondary structures in prokaryotic transcription.

The *E. coli* bacteriophage N4 is the one system known to date that has been shown directly to utilize a cruciform structure in the regulation of the transcription of its early genes. Generally, a hairpin resulting from a short, inverted repeat is stabilized and used as a recognition site for promoter binding and initiation of transcription [reviewed in Wadkins 2000]. Hairpin-forming sequences similar to those in N4 are conserved in a number of other prokaryotes and eukaryotes [Dai 1998]. And, whereas protein binding of ssDNA has an enhancing effect upon transcription as suspected in human *c-myc*, binding of the highly conserved Y box factor upstream in a certain human gene induces the formation of ssDNA and inhibition of transcription from the respective promoter [reviewed in Wadkins 2000]. So, this ssDNA extrusion may either enhance or suppress transcription specific to the regulatory system.

The aforementioned studies indicate that the recognition of ssDNA by proteins may be fundamental to transcription regulation and perhaps even in replication or recombination. Protein-ssDNA interactions in upstream regions may incite the extrusion of other ssDNAs to be bound in promoter regions, for example, in a cooperative cascade. In this way, the secondary structures that likely form from this ssDNA serve as vital means for the direction of protein components. Because of the above evidence for hairpin/cruciform formation in transcriptional regulatory regions as well as other studies for binding of transcription factors and inhibitors to hairpins and further examples of hairpin recognition [reviewed in Wadkins 2000], our lab considers the hairpin/cruciform structure “a potentially important component of regulation of gene expression that might be exploited for drug development” [Wadkins 2000]. Small molecules that specifically interacted with the stem and loop of such structures could have better selectivity with less base coverage than dsDNA-binding agents. Hairpin-selective drugs could either be made to bind to and stabilize hairpins for enhancement of transcription as in mechanisms such as the N4 bacteriophage, or else interact to destabilize the hairpin or offer competition for binding of it as may be desired to fight viruses that may depend on hairpin-like DNA secondary structures for viral replication [South 1993]. Actinomycin D is used as an antibiotic, antitumor agent, and transcription inhibitor and has been shown to recognize and bind portions of the stem and loop of hairpin/cruciform structures [reviewed in Wadkins 2000]. Another study found that the ssDNA-specific cleavage DNA of cells in the mitosis phase by S1 and mung bean nucleases is increased by ten over the same cells in interphase [Juan 1996]. Given that this is due to hairpin formation during mitosis, hairpin-targeted drugs could be tweaked to fight the proliferation of tumors. Therefore,

additional knowledge of molecular recognition and effects upon formation of secondary structures is a worthwhile pursuit.

1.2 Systemic Considerations

Global DNA topology is necessarily more complicated due to the interplay of at least the ionic environment, level of supercoiling, and number and variety of bound proteins. Salt concentration is directly responsible for the gross thermodynamic stability of the helix. Lower monovalent cation levels facilitate extrusion of ssDNA; when less of the negative charge of the DNA molecule is neutralized, it contributes to repulsion between the negatively charged phosphate groups in the backbones of each molecule [Bowater 1994]. On the other hand, divalent cations, namely Mg^{2+} , increase negative DNA supercoiling *in vivo* [Vologodskaja 1999]. Additionally, the superhelical density of the molecule determines the torsional energy required, favoring extrusion of a cruciform structure and concurrent relaxation of negative supercoils; that is, a threshold number of negative supercoils must be crossed for the transition [Oussatcheva 2004].

Overall geometry of the DNA molecule may be altered so that regions of various proximities may be brought near [Vologodskii 1992; 1994; 1999]. Notably, genetic events including DNA replication, control of gene expression through loop formation, transposition, and site-specific recombination, all depend upon communication among proteins bound to distant DNA sites [reviewed in Oussatcheva 2004]. Oussatcheva *et al.* manipulated the position of inverted repeats with respect to permanent bends within plasmids in order to show that the global structure of the DNA molecule effectively alters the level of supercoiling necessary for the helix-cruciform transition [2004].

Correspondingly, the interactions of local DNA structures (via global topology) may modulate the formation of DNA secondary structures, serving as a potential regulatory mechanism for processes that depend on supercoiling, mentioned above. The deficiency of helical turns in negatively supercoiled DNA, and the associated noncanonical secondary structures that may result, reveals the flexibility and dynamic nature of DNA, which is controlled by environment and DNA-binding proteins. Rather than just a linear strand of code, DNA actively varies its 3D conformations to regulate protein access to, and thus expression of, the genetic code defined by the linear sequence of bases.

1.3 Base Methylation

Modification of the adenine and guanine DNA bases is another means by which the DNA stores or otherwise communicates some information to proteins that would act upon it. In *E. coli*, the mismatch proofreading system distinguishes the nascent strand shortly after replication by its lack of methylation of adenine residues. Only some time after the adenine has been incorporated does the deoxyadenine methyltransferase, or methylase, (*dam*) introduce a methyl group to the N⁶ amine in the (5')GATC sequences. These newly formed and unmethylated GATCs allow the new strand to be distinguished for some time so that mismatches can be removed. Such sequences are concentrated in the origin of replication, and only after the newly synthesized A nucleotides in this region have been methylated (a “refractory period” of about ten minutes) can further initiation occur. In vertebrates, methylation of cytosine residues in the sequence CG seems to provide a mechanism for distinguish the active or inactive state of genes. Daughter strands directly inherit this pattern of methylation, and a correct methylation pattern has

been shown crucial to normal murine development. Methylated DNA-binding proteins in vertebrates interact with chromatin-condensing proteins reinforcing transcriptional repression of that gene. Though established by other mechanisms, its inactivity seems to be ensured by DNA methylation. Importantly, DNA methylation maintains the integrity of the vertebrate genome by silencing the transposable elements, which can comprise a significant portion of its sequence. DNA methylation is also used in mammalian cells to distinguish the parental origin of the gene in the case of genomic imprinting [Alberts 2002]. Hypermethylation of cytosine residues in CpG is even characteristic of cancer cell lines in mammals [Araujo 1998]. Though little is known about phenotypes that may result from *dcm* activity in *E. coli*, it is thought to impart protection against certain restriction endonucleases [Palmer 1994].

Might methylation have any effect upon DNA structures, whether locally or globally? Early studies implicated methylation in greatly affecting DNA-protein interactions, as in the aforementioned binding of restriction enzymes [Yuan 1970]. Work in the 1980s showed that cytosine methylation stabilizes left-handed DNA [Behe 1981]. Base methylation can change the thermal stability of the double helix [reviewed in Murchie 1989]. Methylated cytosine residues increase helical stability, while methylated adenines destabilize the helix [Collins 1987] (Figure 3).

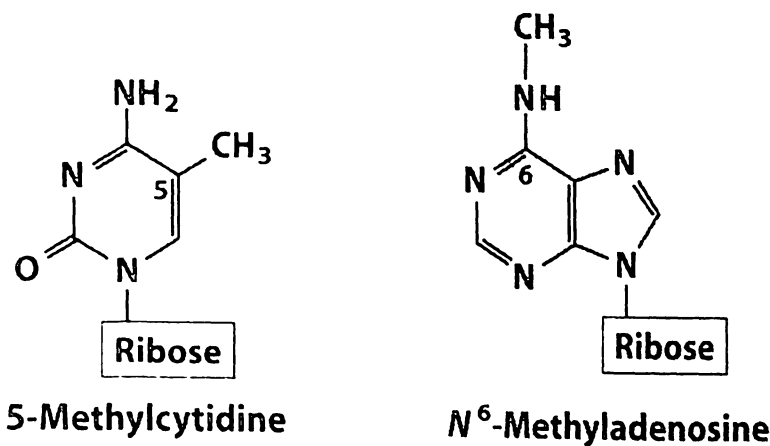


Figure 3: Methylated Nucleotides. Source: Nelson, D. L.; Cox, M. M. Leninger Principles of Biochemistry, 4th ed. New York: W. H. Freeman and Co., 2005. Figure 8-5a. Deoxycytosine methylase (*dcm*) may add a methyl group to the C-5 position on the cytosine nucleotide base, stabilizing the DNA double helix through stacking (left). Deoxyadenine methylase adds the group to the N⁶ amine on the adenine nucleotide, which hinders hydrogen bonding with thymine and therefore decreases helix stability (right).

Lilley has, in several studies, shown that cruciform extrusion is sensitive to local helix stability since the extrusion of a majority of cruciforms begins with helix opening at the center of inverted repeats [reviewed in Murchie 1989]. Small changes in the central sequence of the inverted repeat in their plasmid pIRbke8 altered the rate of cruciform extrusion by a range of 2000 times from slowest to fastest [Murchie 1987]. Murchie and Lilley, prominent early investigators of cruciform dynamics, studied the effect of base methylation on the rate of cruciform extrusion by introducing either N⁶-methyladenine or 5-methylcytosine at the centers of inverted repeats and noting the alterations in extrusion rates. Interference of the hydrogen bonding between adenine and thymine by

methylation of the adenine at the N6 amine facilitates the mechanism for ssDNA extrusion in which base pairing was lost in what would become the unpaired loop region; conversely, methylation of cytosine at C-5 actually leads to an increase in local helical stability through stacking of the nonpolar group between base pairs [Murchie 1989]. Previous evidence suggests a definitive role for base methylation in both local and overall DNA helix stability. No studies to date have examined whether global methylation influences the local or global tertiary structure as another possible regulatory mechanism in the formation of cruciforms.

1.4 Aims and Approach

Generally, the interdependence among supercoiling, ssDNA, and DNA methylation and their regulatory roles in DNA replication and gene expression are acknowledged but not fully explored. Our lab aimed to examine whether gross methylation of respective cytosine and/or adenine nucleotides significantly affects the extrusion of ssDNA to form DNA secondary structures, via changes in either level of supercoiling or general DNA conformation. We questioned whether some shift in global topology due to accommodation of the methyl groups might result in the alteration of helical integrity. Using plasmids from three methylation-state variant strains of a bacteria and ssDNA-specific restriction endonucleases, we compared gross ssDNA content among them. We then compared relative responses of the three to intercalator addition in search of any more quantitative or qualitative differences among the plasmids.

1.4.1 Topology Review

Both strands of DNA are coiled around an axis as a double helix containing about 10.5 base pairs per helical turn in typical B-form DNA, when no supercoiling is present. Coiling of this axis upon itself induces supercoiling. Small closed circular DNA molecules (ccDNA), such as plasmids, are almost always supercoiled, depending upon and characteristic of cell origin. Topological properties, such as the linking number, Lk (number of helical turns in ccDNA), are those that do not change as long as there are no strand breaks; a discontinuous molecule renders Lk undefined. Lk is always an integer and, in a right-handed helix such as B-DNA, is positive. Cells underwind, or decrease Lk , of their DNA as a form of stored energy (Figure 4). The strain is accommodated by supercoiling, which is usually more energetically favorable than the alternative of strand separation and the accompanying hydrogen bond breakage. This accommodation is often measured as Wr , for writhe, and adds to another structural component twist (Tw), which describes the spatial relationship of neighboring bases, to give Lk (Figure 5).

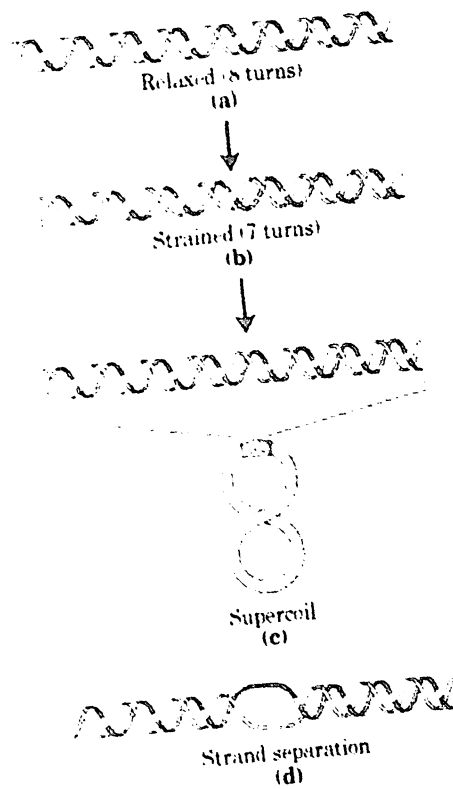


Figure 4: Accommodation of Decreased Lk by Supercoiling. Source: Nelson, D. L.; Cox, M. M. Leninger Principles of Biochemistry. 3rd ed. New York: W. H. Freeman and Co., 2000. Fig 24-13. Underwinding of the DNA molecule by endogenous proteins is compensated by negative supercoiling if strand separation is not stabilized in some other way.

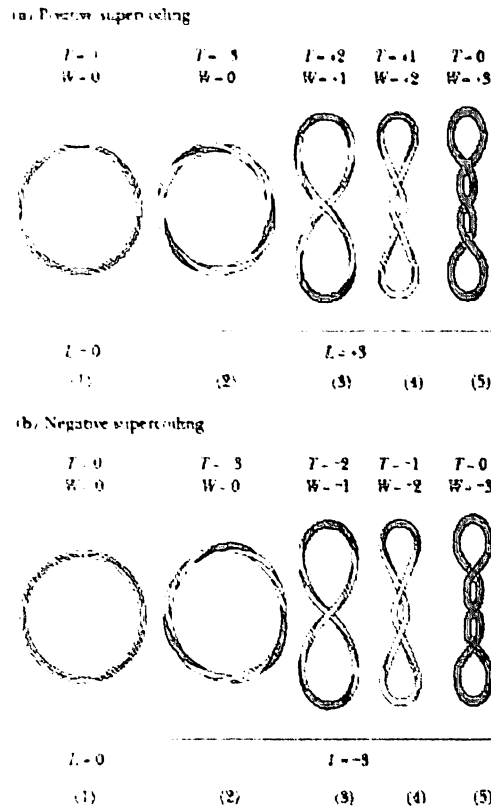


Figure 5: Illustration of Topological Concepts and Terms. Source:

<http://www.web.virginia.edu/Heidi/Chapter12/Images/>. The relaxed circle in 4(b)(2) has

left-handed coiling (three twists) and can be compared to an underwound bacterial plasmid. The stress is relieved by an equivalent number of negative supercoils, as shown in 4(b)(5).

Changes in Lk may also be expressed as σ (superhelical density or specific linking difference), a measure of the change in Lk relative to Lk of relaxed DNA that is irrespective of total number of bases. Most cellular DNA is underwound by about 6%, for a $\sigma = -0.06$. Such a molecule is manifest as right-handed and negatively supercoiled [Nelson 2005].

1.4.2 Experimental System

We chose *E. coli* pBR322 as our model plasmid because it exhibits prominent cleavage by ssDNA specific endonuclease at palindromic sequences in regulatory regions. Sheflin demonstrated that mung bean nuclease reliably cleaves most frequently and intensely in the terminator region of the Amp-R cassette, which is highly enriched in A+T nucleotides compared to that of the pBR322 genome [Sheflin 1985]. Resulting linear DNA fragments can be measured through gel electrophoresis.

Due to differences in charge density, topoisomers from a given plasmid (ccDNA) may be separated into discrete bands based on migration during agarose gel electrophoresis; i.e. a more supercoiled molecule travels faster than a more relaxed molecule of the same size. Our variant strains differed in methylation, not in number of base pairs, and thus were compared with regard to patterns of supercoiling.

MATERIALS AND METHODS

2.1 Plasmids

Wild type *E. coli* K-12 (defective genes/genotype: *F- ara-14 leu flhA2 Δ(gpt-proA)62 lacY1 glnV44 galK2 rpsL20 xyl-5 mtl-1 Δ(mcrC-mrr)_{HB101}*) contains active DNA cytosine methylase (*dcm*), responsible for methylation of internal cytosine residues in the sequences (5')CCAGG and (5')CCTGG [Marinus 1973; May 1975] at the C⁵ position, and DNA adenine methylase (*dam*), which methylates the N⁶ position of adenine residues in the sequence (5')GATC [Marinus 1973; Geier 1979]. pBR322 from this strain were purchased from New England BioLabs, Inc. (Beverly, MA, USA). For additional K12 strain plasmids, XL10-Gold Ultracompetent Cells (Stratagene [La Jolla, CA, USA]) were transformed using the same pBR322 and following the transformation protocol in the QuikChange[®] XL Site-Directed Metagenesis Kit Instruction Manual (Stratagene). Aliquots of 45 μl of ultracompetent cells were transformed using 0.2 μl electrophoresis grade 2-mercaptoethanol (Fisher Scientific) and .01 ng pBR322. The reaction was incubated on ice for 30 minutes, then heat-pulsed in a 42°C water bath for 30 seconds, then again on ice for 2 minutes. We then added 0.5 ml preheated NZY+ broth and incubated at 37°C for 1 hour with shaking at about 250 rpm. We then placed 250μl of transformation reaction onto a LB-Ampicillin Agar plate and incubated at 37°C overnight. We used the QIAGEN[®] Plasmid Mega Plasmid Purification Kit, following instructions in the accompanying handbook (June 2005). Two to three colonies were chosen from the selective plate, and a starter culture of 5 ml LB-ampicillin was inoculated from each and incubated overnight at 37°C with vigorous shaking. We then

diluted one of the starter cultures 1/500 into 2.5 liters of selective medium and incubated at 37°C overnight with vigorous shaking. We then harvested the cells by centrifugation at 6000 x g for 15 minutes at 4°C. The pellet was resuspended in 50 ml of the supplied Buffer P1 (see Section 2.4 for this and subsequent buffer and growth media compositions). An equal volume of Buffer P2 was added, and the lysis mixture was inverted vigorously 4-6 times and incubated at room temperature for 5 min. We added 50 ml of chilled Buffer P3, mixed immediately as before and incubated on ice for 30 min. We centrifuged at 20000 x g for 30 min (or until clear) at 4°C and promptly removed the supernatant containing the plasmid DNA. We then applied the supernatant to the QIAGEN-tip 2500 (previously equilibrated with 35 ml Buffer QBT) and allowed it to filter by gravity. We washed the QIAGEN-tip with 200 ml of Buffer QC and eluted the DNA with 35 ml of Buffer QF. We precipitated the DNA with 24.5 ml room-temperature isopropanol, mixed, and centrifuged immediately at 15000 x g for 30 min at 4°C. The supernatant was decanted. The DNA pellet was then washed with 7 ml of room-temperature 70% ethanol and centrifuged at 15000 x g for 10 min at 4°C. Again, the supernatant was decanted and discarded. The pellet was air-dried for 15 min and redissolved in 200 µl TE buffer, pH 8.0. The DNA concentration was determined by UV spectrophotometry using the CARY 50 Probe. Assuming $A_{260}=50 \mu\text{g ml}^{-1}$ for DNA, we calculated an average 4.2mg ml^{-1} K12 plasmid DNA in our stock sample. The plasmid was stored at 4°C.

E. coli BL21 (DE3) Competent cells (defective genes/genotype: *E. coli* $B^- F^- dcm^- ompT hsdS(rB^- mB^-) gal \lambda(\text{DE3})$) were ordered from Stratagene. The BL21 strain codes for a defective *dcm* gene, designated hence as *dcm*⁻, so that only respective adenines are

methylated. Resulting plasmids may also be referred to as *hemimethylated*. We began the transformation of these cells with 0.5 ng K12 plasmid (produced above) and followed the same protocol as given for transformation and plasmid DNA purification.

Concentration was determined with UV-VIS to be about 3 mg ml⁻¹.

E. coli K12 ER2925 cells (defective genes/genotype: *ara-14 leuB6 fhuA31 lacY1 tsx78 glnV44 galK2 galT22 mcrA dcm-6 hisG4 rfbD1 R(Δgb210::Tn10)TetS endA1 rpsL136 dam13::Tn9 xylA-5 mtl-1 thi-1 mcrB1 hsdR2*) were ordered from New England BioLabs, Inc. This strain contains defective *dcm* and *dam* genes, denoted *dcm*'*dam*', so that methylation at respective cytosine and adenine nucleotides is abolished. Resulting plasmids will be termed *unmethylated*. In order to grow a culture of this strain for more high-efficiency transformation, we inoculated 5 ml of nonselective LB with 1 μl bacteria and incubated at 37°C overnight with shaking. We then followed the Inoue Method for "Ultra-Competent" *E. coli* [1990]. We inoculated 250 ml SOB with all 5 ml and incubated at room temperature overnight. We then iced the culture for 10 minutes and centrifuged it at 2500 x g for 10 min at 4°C. We then resuspended the cells gently in 80 ml of ice cold TB and iced for 10 min. We centrifuged again at 2500 x g for 10 min at 4°C and resuspended the pellet gently in 20 ml of ice cold TB. DMSO was added to a final concentration of 7%. The cells were chilled on ice for 10 min, then aliquoted into 2 ml and stored at -70°C. In order to produce our unmethylated plasmid, 1.0 ng K12 *wt* pBR322 (from amplification) was required for transformation of 50 μl ER2925 "ultra-competent" cells. Transformation protocol was then followed as above to yield about 3 mg ml⁻¹ plasmid DNA. The plasmid was then stored at 4°C in TE buffer.

2.2 Endonuclease Restriction

Mung bean nuclease reaction protocol was adapted from Sheflin and is as follows [1985]. Reaction mixtures contained 10 mM Tris-HCl and 1mM Na₂EDTA (pH 7.0) and 0.8 µg pBR322 plasmid DNA in a volume of 16 µl. Mung bean nuclease (MBN) is a single-strand specific DNA endonuclease that degrades single-stranded extensions (hairpin loops) and was ordered from New England BioLabs Inc. at 10000 units/ml. We added 0.8 µl undiluted (8 units) MBN to the mixture, which was incubated at 37°C for 1 hour. The reaction was then stopped with 40 mM Tris (pH 11.7), 2 mM magnesium acetate, and 0.01 % Triton X-100, for a final volume of 37 µl. Initially, 3 µl of 42 unit/mgDW venom phosphodiesterase (Worthington Biochemical Corp., Lakewood, NJ, USA) was added (and incubated at 37°C for 10 minutes) at this point to cleave opposite the mung bean nicks, but was later found unnecessary. The solution was extracted twice with an equal volume of phenol:chloroform (1:1). The aqueous layer was transferred each time to a new microcentrifuge tube. The DNA was then precipitated with 110 µl (3x volume before extraction) of ice cold 95% ethanol and centrifuged at maximum speed in a benchtop microcentrifuge for 20 minutes at room temperature. The supernatant was carefully removed, and the remaining DNA was then air-dried in the fume hood for 15 minutes to evaporate the remaining ethanol. The DNA pellet was then resuspended in 1x Hind III buffer and 1 µl (20 units) of Hind III restriction endonuclease (New England BioLabs, Inc.) was added for a total reaction volume of 20 µl. The reaction was then incubated for one hour at 37°C. We added 1x loading buffer, and 1% agarose gel electrophoresis was performed at about 23V overnight in 1x TAE buffer.

The gel was then stained with 1x SYBR[®] Green I nucleic acid gel stain (Invitrogen) for at least one hour before imaging with the BIO RAD Gel Doc Transilluminator. A control mixture for Hind III digestion and one with no restriction enzymes were simultaneously prepared and imaged. A similar mass of 2-Log DNA ladder (0.1-10.0 kb; New England BioLabs, Inc.) was included in electrophoresis as a molecular weight standard for the linearized DNA.

2.3 Topoisomer Production

A range of topoisomers of each strain were produced by an adapted protocol from Keller, as follows [Keller 1975]. Each reaction mixture contained 0.8 μg plasmid DNA in a total volume of 100 μl "Topo" buffer. The DNA intercalator ethidium bromide (Sigma) was added to the mixtures in concentrations ranging from 0—0.07 mol(mol base pairs)⁻¹ (see gel figures captions for values). Each sample was then treated with 6 units of Human Topoisomerase I (TopoGEN). A control mixture was included which did not contain Topoisomerase I and ethidium bromide (EtBr). After incubation at 37°C for 1 hour, the mixtures were extracted twice with phenol:chloroform (1:1) at 37°C. The aqueous phase was recovered and transferred to a new tube. The DNA was then precipitated with ice cold 95% ethanol and centrifuged at maximum speed in a benchtop centrifuge for 20 minutes. The DNA pellets were air-dried and dissolved in 50 μl TE. Aliquots of 23 μl were analyzed by 1% agarose gel electrophoresis at about 23V overnight in 1x TAE buffer. Alternatively, gel electrophoresis was performed with 1% agarose gel and electrophoresis buffer each containing 0.012 $\mu\text{g ml}^{-1}$ EtBr. After destaining overnight in 1x TAE, gels were then stained with 1x SYBR[®] Green.

Subsequent imaging was performed on the UV transilluminator, as before. Analysis of gel images was performed using ImageJ software, and KaleidaGraph was used to plot data.

2.4 Buffers and Media

NZY+ Broth (per liter): 10g of NZ amine (casein hydrolysate); 5 g of yeast extract; 5 g of NaCl; add deionized H₂O to a final volume of 1 liter; adjust to pH 7.5 using NaOH; autoclave; and add the following filter-sterilized supplements prior to use: 12.5 ml of 1 M MgCl₂, 12.5 ml of 1 M MgSO₄, and 20 ml of 20% (w/v) glucose (or 10 ml of 2 M glucose).

LB liquid (per liter): 10 g of NaCl; 10 g of tryptone; 5 g of yeast extract; add deionized H₂O to a final volume of 1 liter; adjust pH to 7.0 with 5 N NaOH; autoclave.

LB Agar (per liter): 10 g of NaCl; 10 g of tryptone; 5 g of yeast extract; 20 g agar; add deionized H₂O to a final volume of 1 liter; adjust pH to 7.0 with 5 N NaOH; autoclave; and pour into Petri dishes (~25 ml/100-mm plate).

LB—Ampicillin Agar (per liter): 1 liter of LB agar; autoclave; cool to 55°C; add 100 mg of filter-sterilized ampicillin; and pour into Petri dishes or as needed [Quik Change, June 2005].

P1: Dissolve 6.06 g Tris base and 3.72 g Na₂EDTA·2H₂O in distilled water to a final volume of 1 liter; adjust pH to 8.0 with HCl; add 100 mg of Rnase A; store at 4°C.

P2: Dissolve 8.0 g NaOH pellets in 950 ml distilled water; add 50 ml 20% SDS (w/v) solution.

P3: Dissolve 294.5 g potassium acetate in 500 ml distilled water; adjust the pH to 5.5 with glacial acetic acid (~110 ml); adjust volume to 1 liter with distilled water.

QBT: Dissolve 433.83 g NaCl and 10.46 g MOPS (free acid) in 800 ml distilled acid; adjust the pH to 7.0 with NaOH; add 150 ml pure isopropanol and 15 ml 10% Triton X-100 solution (v/v); adjust the volume to 1 liter with distilled water.

QC: Dissolve 58.44 g and 10.46 g MOPS (free acid) in 800 ml distilled acid; adjust the pH to 7.0 with NaOH; add 150 ml pure isopropanol; adjust the volume to 1 liter with distilled water.

QF: Dissolve 73.05 g NaCl and 6.06 g Tris base in 800 ml distilled water; adjust pH to 8.5 with HCl; add 150 ml pure isopropanol; adjust the volume to 1 liter with distilled water.

TE: 10 mM Tris·Cl, pH 8.0; 1 mM EDTA [Qiagen Plasmid Purification Handbook, June 2005].

SOB: 2% (w/v) bacto tryptone, 0.5% (w/v) yeast extract, 10 mM NaCl, 2.5 mM KCl, 10 mM MgCl₂, 10 mM MgSO₄, pH 6.7 – 7.0.

TB: 10 mM PIPES, adjust pH to 6.7 with 5 N KOH; 55 mM MnCl₂, 15 mM CaCl₂, 250 mM KCl [Inoue 1990].

RESULTS

The three *E. coli* pBR322 methylase-state variant plasmids K12, BL21, and ER 2925, are all 4361 bp, supercoiled ccDNAs characterized by intact DNA adenine and cytosine methylases (*wt*), defective cytosine methylase (*dcm*⁻), and nonactive methylases (*dam*⁻/*dcm*⁻), respectively. While all possible sites in the plasmid may not be methylated, there exist 22 of the adenine methylase recognition sequences [Bergerat 1989] and 6 DNA cytosine methylase sites [rebase.neb.com] within the pBR322 plasmids. Four potential adenine methylation sites exist proximal to the region that Sheflin found was most intensely cleaved by MBN [1985] (Figure 6). Note the prominence of adenine and thymine bases, which are bound by two hydrogen bonds and are less stable than the three hydrogen bonds between cytosine and guanine bases. Also contained in this short sequence within the terminator of the Amp-R gene is the highlighted palindromic sequence, which has the potential to form a substantial cruciform structure subsequent to melting out of ssDNA in this region.

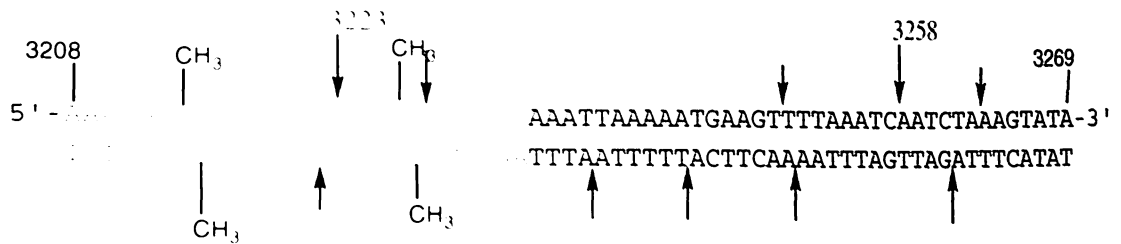


Figure 6: Area of Interest in Terminator Region of Amp-R Gene. Source: Adapted from Sheflin, L. G.; Kowalski, D. *Nucleic Acids Res.* **1985**, *13*, 6137-6154. Arrows indicate frequent MBN cleavage sites in the pBR322 plasmid; longer arrows indicate increased frequency of cleavage, and the sites in red are the two most prominent restriction sites as shown by Sheflin. Sites of possible nucleotide methylation are noted. The highlighted area (green) is a palindromic sequence and contains both methylation sites and one of the prominent ssDNA-specific restriction sites.

3.1 Mung Bean Nuclease Cleavage Patterns Among pBR322 Variant Plasmids

Initially, supercoiled pBR322 DNA was nicked with the ssDNA specific MBN, then linearized by cleavage opposite the nick using venom phosphodiesterase (VPD), as prescribed by Sheflin [1985]. However, we showed that VPD treatment was unnecessary to linearize the DNA and even had the effect of fully cleaving the plasmid without the MBN (results not shown). Therefore, we omitted VPD from subsequent MBN reactions. After reaction with MBN, the resulting fragment was cut using the HindIII endonuclease. In this way, a pair of fragments will result whose lengths add up to 4361 bp (Figure 7).

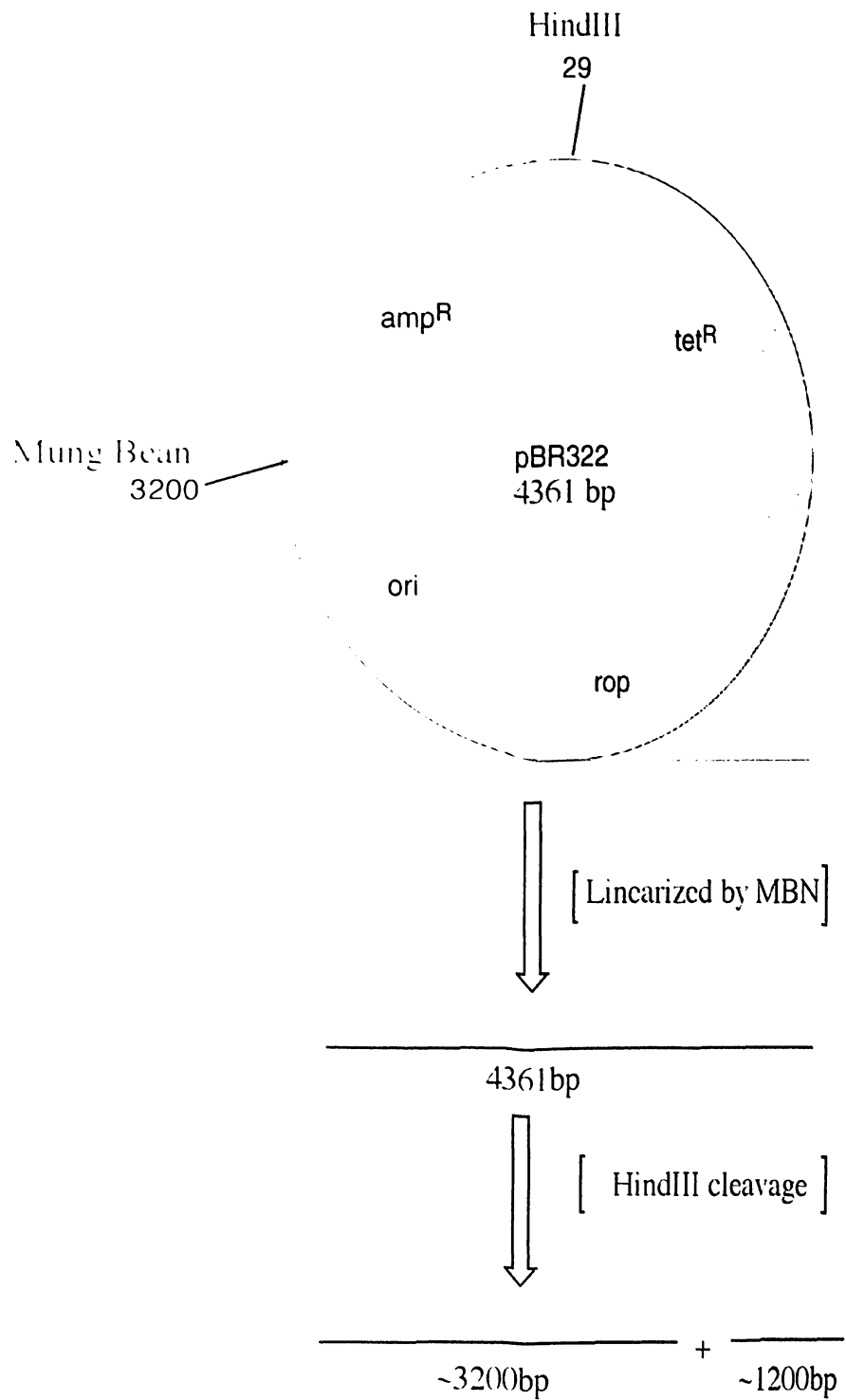


Figure 7: Basic Map of pBR322 Plasmid and Restriction Products. The circular plasmid is cleaved first by MBN—if ssDNA is present—to yield a linear DNA molecule and then by Hind III to identify the general site of the first cleavage.

These linear products are separated on the basis of size by agarose gel electrophoresis; smaller bands are more mobile through the agarose matrix in the presence of an electrical current and are conventionally at the bottom of a gel image. As shown below, all three strains exhibit cleavage indicative of digestion by MBN and Hind III, such that methylation state does not seem to have a significant effect upon the formation of ssDNA at the prominent MBN site (Fig. 8; lanes 3, 6, and 9). The discreet banding pattern indicates that the nicks occur at specific sites. Intensity variations of the bands are relative to frequency of cleavage that produce those size fragments and vary somewhat with amount of DNA recovered at the end of the reaction. The 2-log ladder to the right can be used to reference fragment lengths. However, circular DNA—closed and supercoiled, closed and relaxed (closed circular), or nicked (open circular)—travels according to spatial charge density and cannot be measured in length according to the marker DNA in the ladder.

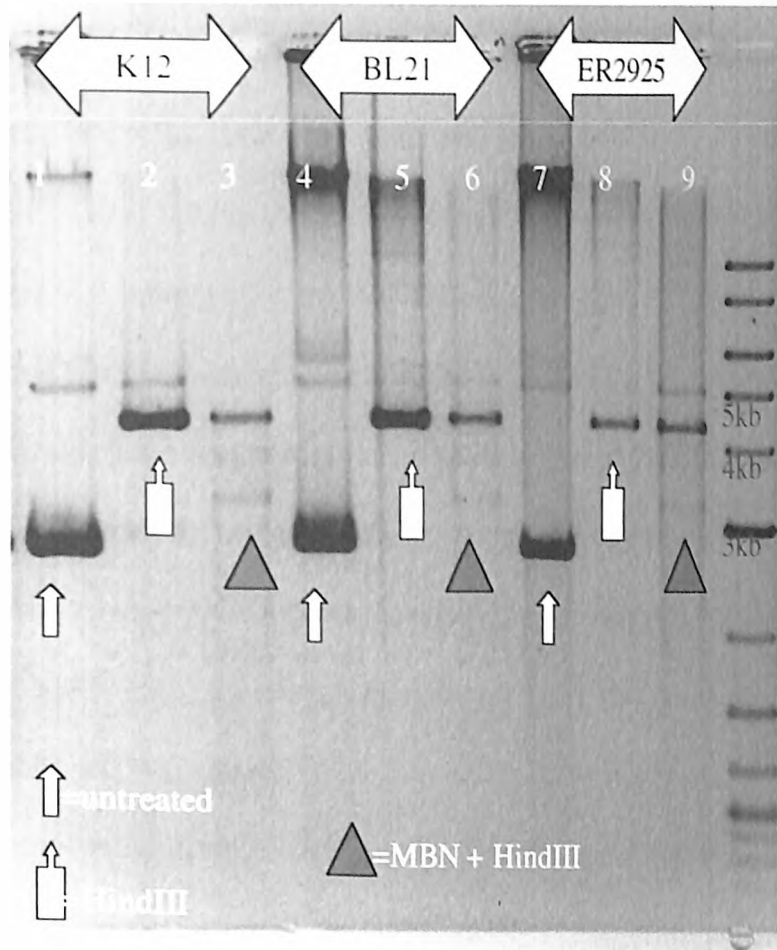


Figure 8: Gel Electrophoresis Image of MBN Digestion Results. As highlighted in lanes 3, 6, and 9, a distinct fragment indicates cleavage by MBN and presence of ssDNA. Lanes 1-3 are K12 strain plasmid, 4-6 are BL21, and 7-9 are ER2925. In each series of three lanes, the first lane is untreated DNA, second is reacted with HindIII alone, and third is reacted with MBN and HindIII. The last lane contains fragments for size reference.

Relaxed DNA with at least one strand of the DNA still intact travels slower than the full-length linear DNA and comes to rest at about the level of the 5.0 kb marker. The naturally supercoiled DNA seen in the lanes with untreated samples is much more compact and travels to a point just below the 3.0 kb marker (lanes 1, 4, and 7). Since the fluorescent stain used for imaging binds to DNA and a "smear" of fluorescence is seen in most lanes, the samples are heterogeneous and contain fragments resulting from physical damage to the DNA *in vitro* or scattered cleavage by the relatively nonspecific sequence recognition of MBN. Using DNA relaxing enzyme (Topoisomerase I, discussed later), we confirmed that MBN does not selectively cleave relaxed pBR322, which would be less likely to extrude ssDNA. Though there is evidence of restriction to a range of fragment sizes, there are no discrete bands produced (gel image not shown). As a procedural note, we chose not to react the MBN and DNA in the MBN buffer as included by the supplier, because of its relatively high monovalent salt concentration that favors conservation of the double helix in the plasmid.

3.2 Topoisomers and Relative Superhelical Conformation

In order to look more closely at any effect of system-wide methylation or lack of methylation upon the pattern of superhelical winding in the three plasmids, we compared their mobilities when relaxed with human Topoisomerase I in the presence of ethidium bromide. Breakage of one strand of DNA, rotation of the other a full turn about its phosphodiester backbone, and reannealing changes the linking number by one and results in a topoisomer of the original. Topoisomerase enzymes regulate the DNA winding state. Type I changes Lk in increments of one by breaking only one of the DNA

strands and allowing for rotation about that strand. This type generally relaxes negative supercoils in *E. coli*. Type II Topoisomerases transiently cleave and rejoin both strands [Nelson 2005]. In prokaryotes, this type is known as gyrase and induces underwinding and corresponding negative supercoils through the hydrolysis of ATP. Gyrase action facilitates helix opening, a requisite for transcription initiation by bacterial RNA polymerase [Alberts 2002].

The aim of comparing possible long distance, or global, effects of base methylation upon the plasmid structures was accomplished by manipulating the number of supercoils in each plasmid using Topoisomerase I (Topo I) for relaxation of the negative supercoils. We manipulated the extent of relaxation, or number of supercoils remaining after reaction with Topo I, by adding various levels of ethidium bromide (EtBr) to the reaction mixtures. Intercalators, such as EtBr, are molecules that bind DNA by inserting a planar aromatic chromophore between base pairs. (Figure 9 illustrates the topological changes and corresponding electrophoretic mobility of increasing concentrations of the addition of such an intercalator.) The addition of EtBr to a negatively supercoiled molecule subsequently induces local unwinding through a decrease in bond angle between neighbors, resulting in a decrease in negative DNA supercoiling and effectively destabilizing any cruciforms present. (Concentration ranges over which intercalators modulate cruciform extrusion also correspond to cytotoxic effects of these DNA-binding drugs *in vitro* [Intercalators].)

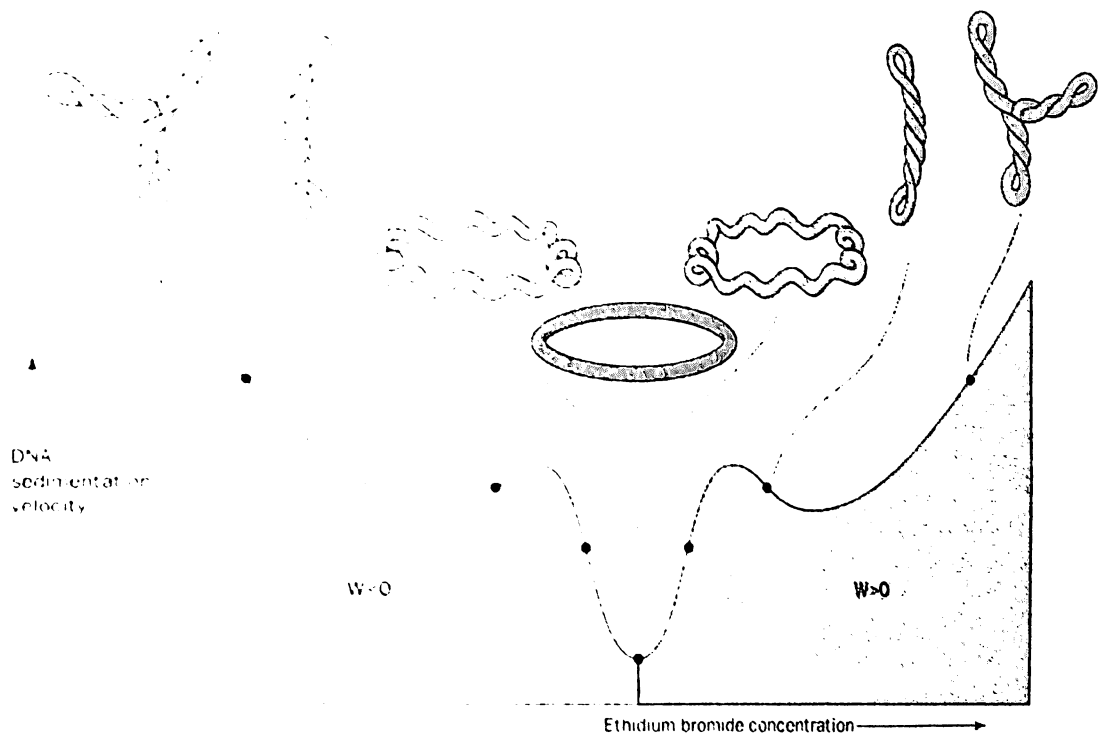


Figure 9: Effect of Intercalator Addition upon ccDNA Topology and Gel Electrophoresis Mobility. Source: Bauer, W.C.; Crick, F.H.C.; White, J.H. *Scientific American*. 1980, 243, 118-129. Highly negatively and positively supercoiled circular DNA molecules travel quickly during AGE. Relaxed molecules travel most slowly. As EtBr is added to negatively supercoiled DNA, the DNA becomes less supercoiled, then relaxed, then more positively supercoiled.

As an example of one of our reaction mixtures and its effect, a relatively small concentration of EtBr compared to number of base pairs of DNA was added to the DNA with an initial t number of supercoils so that lesser n supercoils remain. The DNA was then effectively relaxed with Topo I. The reaction was stopped and both the EtBr and Topo I were removed by extraction to leave a ccDNA with $(t-n)$ supercoils, which would travel more quickly during gel electrophoresis than an equal amount of DNA relaxed in the presence of more EtBr, but less quickly than naturally supercoiled plasmid.

Since topoisomers resolve as discrete bands with differing electrophoretic mobilities, a stair step of increasing superhelical density could be constructed by the addition of more EtBr to the DNA before its relaxation with Topo I. As shown by Depew and Wang [1975] and by Pulleyblank *et al.* [1975], thermal fluctuation in the DNA helix at the time of ring closure causes heterogeneity in the number of supercoils of the resulting ccDNA. Each DNA sample, then, contains a set of molecules differing in supercoiling in a Gaussian-type distribution around a mean value. If the differences in σ of samples in neighboring lanes are not too large, the distribution of bands will overlap; those with the same electrophoretic mobility are also equivalent in σ [Keller 1975].

As seen in the gel below, lane 1 contained no EtBr and migrates most slowly as a completely relaxed ccDNA. This lane, therefore, sets the zero for superhelical density for the fully methylated strain. Subsequent lanes from left to right increase in the number of supercoils corresponding to the number of bands from lane 1 to the average peak of lane 2, and so on (Figure 10). Lane 6 contains untreated DNA; the upper band is nicked DNA and the lower naturally supercoiled. This latter set of molecules appears to form a single band but is, in fact, a similar distribution of highly supercoiled DNA that migrates too quickly for the resolution of this gel. There is no overlap of neighboring bands between lanes 5 and 6, and one cannot count the increase in number of supercoils between these two samples to measure the σ of the plasmid DNA.

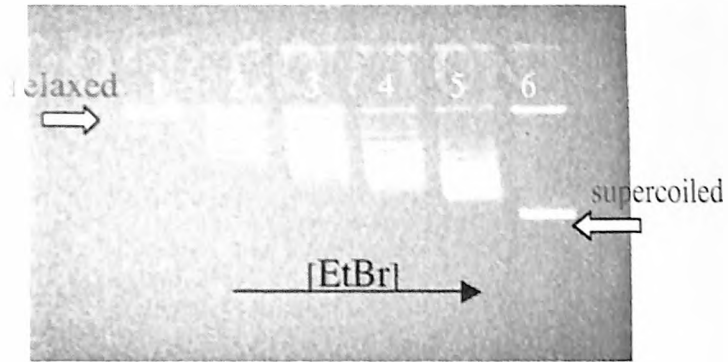


Figure 10: Gel Image of Topoisomer Production in K12 pBR322. Note the effect of increasing EtBr concentration during relaxation with TopoI (not to be confused with the simple addition of EtBr illustrated in Figure 8).

A small concentration (0.012 $\mu\text{g/ml}$) of EtBr was added to the agarose gel and electrophoresis buffer, and another approximately 250 μg aliquot of the same pBR322 K12 plasmid reaction mixtures was analyzed in this electrophoresis condition. The added EtBr essentially “rescaled” the gel resolution range by partially relaxing the very supercoiled lane 6 so that its topoisomers could be imaged and compared to those in lane 5, as described (Fig. 11). Lanes that contained relaxed DNA before the addition of EtBr to the gel (such as lane 1), had increased mobility in Figure 11 because they had been made positively supercoiled by the intercalator (recall Fig. 9).

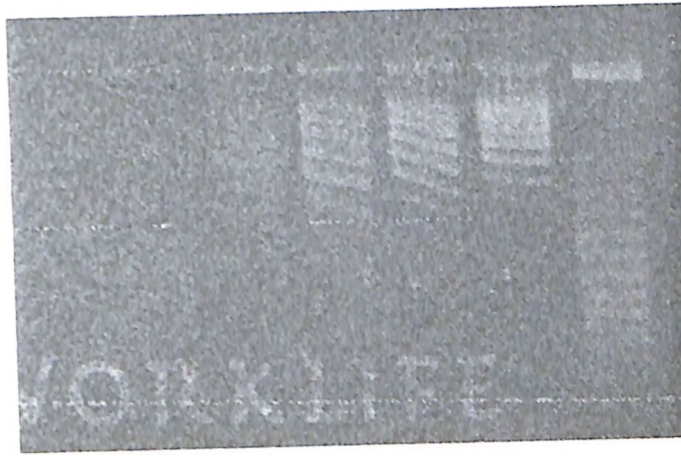


Figure 11: Gel Image of Topoisomer Production in K12 pBR322 + EtBr.

This DNA is from the same reaction mixture as Figure 10, but with the addition of 0.012 $\mu\text{g/ml}$ EtBr gel conditions. The highly supercoiled, untreated DNA in lane 6 is, in this way, resolved into its component band set of topoisomers.

We used ImageJ software to analyze the average intensity location of each component band set in order to find the midpoint of the distance traveled by each (Figure 12). When plotted one above/below its neighbor, the difference between different DNA samples in the mean number of supercoils were counted directly in units of turns, since adjacent peaks are separated by one superhelical turn. We estimated an error of about ± 0.5 -1.0 turn for each individual comparison. By simple visual inspection of the band overlaps between lanes 1-3 and 3-5 from Figure 10 and lanes 5-6 in Figure 11, there are approximately -16 ± 3 superhelical turns. Since the Lk for pBR322 should be 415 in its relaxed state, 16 negative supercoils create a σ of about -0.0385.

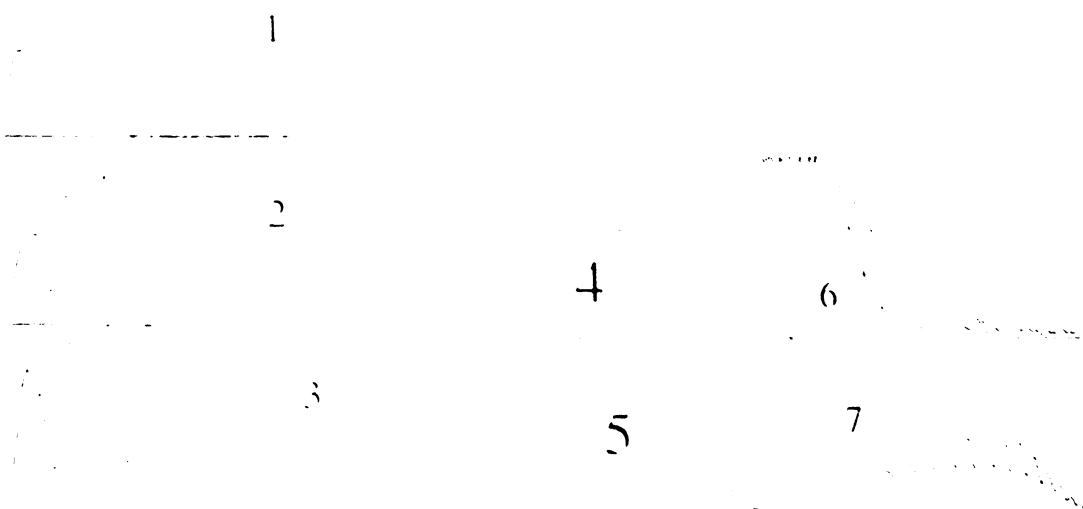


Figure 12: Relative Intensity/Mobility Tracings of Topoisomers from K12 pBR322. Tracings 1-5 are of respective lanes in Figure 9, and 6 & 7 are from lanes 5 and 6 in Figure 10. Note that tracings 5 and 6 contained the same [EtBr] during reaction with Topo I. Measurements were made from points of average mass/intensity.

As seen in gel electrophoresis images of the *dcm⁻* and *dcm⁻/dcm⁻* strains (Fig. 13), however, we were unable to resolve the discrete component band sets even with multiple attempts. In order to make a comparison, then, of variability of supercoiling with added EtBr among the three strains, we subsequently compared changes in [EtBr] with relative distance traveled by the midpoint of each band distribution. Using the distance from the linear genomic DNA (top band of gels) to ccDNA/nicked DNA (next band down) as the standard (0 - 1.0), we measured the distances from the midpoint of the intensity of the relaxed DNA (lane 1; zero distance) to the midpoint of subsequent bands. Gels containing EtBr were needed as before in order to produce the continuous downward digression toward the untreated DNA, and distance values were expressed as fractions of the standard distance.

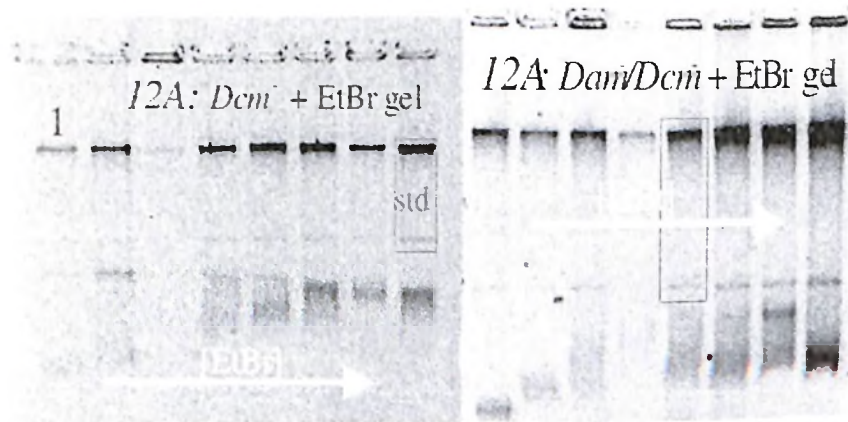


Figure 13: Gel Images of Topoisomer Production in *dcm*⁻ and *dam*⁻/*dcm*⁻ pBR322. The gel shown in 13A contains BL21 strain plasmid reacted with TopoI in the presence of increasing [EtBr] and EtBr electrophoresis conditions. Gel 12B contains plasmid from the ER2925 strain similarly reacted and processed. The same electrophoretic mobility trend as in K12 strain is also seen in these two strains, but without resolution of individual topoisomers. The highlighted box in each outlines the standard for distance (genomic → relaxed = 1.0).

Measurements from gel electrophoresis images of all three pBR322 strains were plotted to give linear fit curves (Fig 14). The slopes of the lines indicate the amount of change effected by intercalator addition to the supercoiled plasmids. Similar slopes were expected for plasmids with equal lengths and more supercoils than our [EtBr] range could relieve. The plasmids, despite presence or exclusion of systemic methylation, seem to share similar 3D conformations with no remarkable deviations in topology.

Supercoiling trend

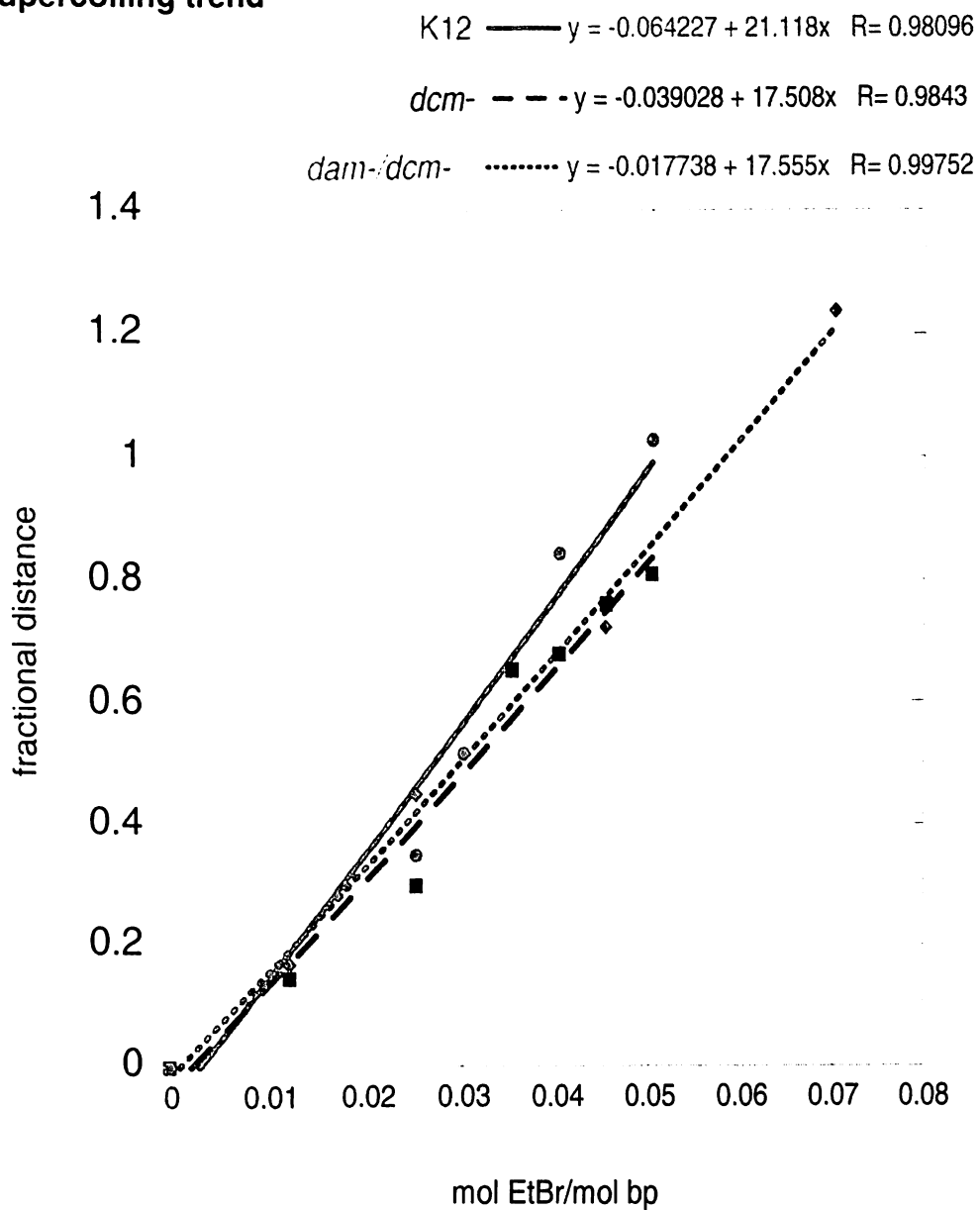


Figure 14: Comparison of Changes in Supercoiling by Intercalator

Concentration. Rate of increase in gel mobility/supercoiling per addition of EtBr before relaxation is uniform among the three methylation-state variants, as indicated by similar slopes.

DISCUSSION

Studies of DNA structure have continued to show surprising interactions among its primary, secondary, and tertiary organization and the consequent biological significance. The underwinding inherent in negatively supercoiled DNA imparts the physical variability that is seen in alternative DNA conformations such as the cruciforms that occur within DNA symmetry elements. These changes in local DNA structure are critically active in various DNA processing events. Local changes are then a significant influence on system-wide structure. Global topology, in turn, may modulate the likelihood of alternative DNA secondary structure formation and its consequent regulatory roles. This complex interplay, though incompletely understood, is considered a regulatory control in gene expression and other supercoiling-dependent events in DNA [Oussatcheva 2004]. In this way, we hypothesized that any significant substitution, addition, or deletion at the molecular level could result in distortion of topology, which would then affect, among other things, cruciform formation and DNA function.

Much more is known now than a couple of decades ago about the factors at work on the secondary and tertiary levels, but many aspects remain unexplored. The results of our studies revealed no conclusive effect exerted by either local or global DNA base methylation or lack thereof upon ssDNA extrusion in bacterial plasmid DNA. Each strain—whether fully methylated, hemimethylated, or unmethylated—possesses at least the threshold level of supercoiling necessary for ssDNA extrusion and the formation of cruciform structures. This finding is reinforced when considering that the 100 bp locality

of the most intense MBN cleavage sites and a large palindromic sequence contains six possible adenine methylation sites. The quantitative limitations of our approach are evident: we observed only the *presence* of bands corresponding to fragment lengths resulting from cleavage by the ssDNA-specific endonuclease. The trend of increasing superhelicity (or electrophoretic mobility) plotted against addition of increasing concentrations of intercalator in the presence of relaxing enzyme is shown as similar curves for the three strains. These data suggest a similar response of each strain to topological change agents—i.e. regular patterns of supercoiling. Overall, our study seems to suggest an insignificant influence of systemic methylation patterns upon cruciform extrusion, whether through local or long distance effects.

Our results were necessarily limited by our simple technical approach toward this investigation. This is evident in the substitution of trend analysis for superhelical density determination because of the inability to number the supercoils (i.e. resolve component band sets of topoisomers) of the *dcm*⁻ and *dam*⁻/*dcm*⁻ strains. A more thorough evaluation of superhelical density and threshold of cruciform extrusion may be informative and can be accomplished through 2D gel electrophoresis [Oussatcheva 2004]. A topoisomer mixture of plasmid that can form an extended cruciform may undergo electrophoresis in the first dimension, as usual, and in the second dimension in the presence of EtBr. In this way, the formation of a cruciform would relieve multiple supercoils and resolve a topoisomer with sufficient superhelical turns as two separate points that overlapped in one of the dimensions. Additionally, plasmids with the same number of positive and negative supercoils could be distinguished in the second condition. Atomic force

microscopy could also be used to actually view sample plasmids for possible cruciforms and any conformational variations.

LIST OF REFERENCES

- Alberts, B., et al. Molecular Biology of the Cell. 4th ed. New York: Garland Science, 2002.
- Araujo, F. D., et al. *Mol. Cell. Biol.* **1998**, *18*, 3475-3482.
- Bauer, W.C.; Crick, F.H.C.; White, J.H. *Scientific American*. **1980**, *243*, 118-129.
- Behe, M.; Felsenfeld, G. *Proc. Natl. Acad. Sci.* **1981**, *78*, 1619-1623.
- Bergerat, A.; et al. *J. Biol. Chem.* **1989**, *264*, 4064-4070.
- Bowater, R. P., et al. *Nucleic Acids Res.* **1994**, *22*, 2042-2050.
- Collins, M.; Myers, R. M. *J. Mol. Biol.* **1987**, *198*, 737-744.
- Dai, X., et al. *J. Mol. Biol.* **1998**, *283*, 43-58.
- Depew, R. E.; Wang, J. C. *Proc. Natl. Acad. Sci.* **1975**, *72*, 4275-4279.
- Geier, G.E.; Modrich, P. *J. Biol. Chem.* **1979**, *254*, 1408-1413.
- Iacono-Connors, L.; Kowalski, D. *Nucleic Acids Res.* **1986**, *14*, 8949-8962.
- Inoue, H.; et al. *Gene* **1990**, *96*, 23-28.
- Juan, G., et al. *Exp. Cell Res.* **1996**, *227*, 197-202.
- Keller, W. *Proc. Natl. Acad. Sci.* **1975**, *72*, 4876-4880.
- Leach, D. R. F. *BioEssays* **1994**, *15*, 893-900.
- Lilley, D. M. J. *Proc. Natl. Acad. Sci.* **1980**, *77*, 6468-6472.
- Lilley, D. M. J.; Gough, G. W.; Hallam, L. R.; Sullivan, K. M. *Biochimie* **1985**, *67*, 697-706.
- Marinus, M.G.; Morris, N.R. *J. Bacteriol.* **1973**, *114*, 1143-1150.
- May, M.S.; Hattman, S. *J. Bacteriol.* **1975**, *123*, 768-770.
- Murchie, A. I. H.; Lilley, D. M. J. *Nucl. Acids Res.* **1987**, *15*, 9641-9654.
- Murchie, A. I. H.; Lilley, D. M. J. *J. Mol. Biol.* **1989**, *205*, 593-602.

- Nelson, D. L.; Cox, M. M. Leninger Principles of Biochemistry, 3rd ed. New York: W. H. Freeman and Co., 2000.
- Nelson, D. L.; Cox, M. M. Leninger Principles of Biochemistry, 4th ed. New York: W. H. Freeman and Co., 2005.
- Oussatcheva, E. A., et al. *J. Mol Biol.* **2004**, *338*, 735-743.
- Palecek, E. *Crit. Rev. Biochem. Mol. Biol.* **1991**, *26*, 151-226.
- Palmer, B.R.; Marinus, M.G. *Gene* **1994**, *143*, 1-12.
- Pearson, C. E. et al. *M. J. Cell. Biochem.* **1996**, *63*, 1-22.
- Platt, J. R. *Proc. Natl. Acad. Sci. USA* **1955**, *41*, 181-183.
- Pulleyblank, D.E.; et al. *Proc. Natl. Acad. Sci.* **1975**, *72*, 4280-4284.
- Sheflin, L. G.; Kowalski, D. *Nucleic Acids Res.* **1985**, *13*, 6137-6154.
- South, T. L.; Summers, M. F. *Protein Sci.* **1993**, *2*, 3-19.
- Vologodskii, A. V. *Topology and Physics of Circular DNA*. Boca Raton, FL: CRC Press, 1992.
- Vologodskii, A. V.; Cozzarelli, N. R. *Annu. Rev. Biophys. Biomol. Struct.* **1994**, *23*, 609-643.
- Vologodskii, A. V.; Cozzarelli, N. R. *Biophys. J.* **1996**, *70*, 2548-2556.
- Vologodskaja, M. Y.; Vologodskii, A. V. *J. Mol. Biol.* **1999**, *289*, 851-859.
- Wadkins, R. M. *Curr. Med. Chem.* **2000**, *7*, 1-15.
- Yuan, R.; Meselson, M. *Proc. Natl. Acad. Sci.* **1970**, *65*, 357-362.